



HAL
open science

Comparison between 0D and 1D approaches for mechanical dissipation measurement during fatigue tests

Pawarut Jongchansitto, Corentin Douellou, Itthichai Preechawuttipong,
Xavier Balandraud

► **To cite this version:**

Pawarut Jongchansitto, Corentin Douellou, Itthichai Preechawuttipong, Xavier Balandraud. Comparison between 0D and 1D approaches for mechanical dissipation measurement during fatigue tests. *Strain*, 2019, 55 (3), pp.e12307. 10.1111/str.12307 . hal-04005028

HAL Id: hal-04005028

<https://uca.hal.science/hal-04005028>

Submitted on 25 Feb 2023

HAL is a multi-disciplinary open access archive for the deposit and dissemination of scientific research documents, whether they are published or not. The documents may come from teaching and research institutions in France or abroad, or from public or private research centers.

L'archive ouverte pluridisciplinaire **HAL**, est destinée au dépôt et à la diffusion de documents scientifiques de niveau recherche, publiés ou non, émanant des établissements d'enseignement et de recherche français ou étrangers, des laboratoires publics ou privés.

Comparison between 0D and 1D approaches for mechanical dissipation measurement during fatigue tests

P. Jongchansitto¹, C. Douellou², I. Preechawuttipong¹ and X. Balandraud^{2,*}

¹ Department of Mechanical Engineering, Faculty of Engineering, Chiang Mai University, 239 Huay Kaew Rd., Muang District, Chiang Mai 50200, Thailand

² Université Clermont Auvergne, CNRS, SIGMA Clermont, Institut Pascal, F-63000 Clermont-Ferrand, France

Abstract

Fatigue in materials is generally associated with the production of heat, leading to the “self-heating” of the tested material. The associated heat power density, named *mechanical dissipation* or *intrinsic dissipation*, can be deduced from the temperature changes captured on the tested specimen’s surface by infrared thermography. When mechanical dissipation is spatially homogeneous in the tested specimen, the processing can be performed using a macroscopic approach, also named zero-dimensional (0D) approach. The latter uses an averaged temperature over the whole specimen’s measurement zone. The present study aims to analyze the error generated by the 0D approach in the assessment of mechanical dissipation. This error was measured with respect to a one-dimensional (1D) approach, which is applicable for longitudinal specimens subjected to uniaxial loading. Experimental tests were performed on pure copper and acrylic glass. A model was also developed to analyze the influence of the material and of the heat exchanges with the specimen’s environment. The results obtained show that the error generated by the 0D approach in mechanical dissipation measurement may not be negligible, and that attention should be paid to the choice of approach for fatigue analysis.

Keywords: fatigue, heat source, infrared thermography, mechanical dissipation, intrinsic dissipation, self-heating, 0D approach, 1D approach

1. Introduction

Material fatigue is generally associated with the production of heat. The term “self-heating” is often used to describe this phenomenon. The associated heat power density (in W/m^3) is named *mechanical dissipation* or *intrinsic dissipation*. The assessment of this calorific quantity is of prime interest in the elaboration of material behavior laws, since it is related to fatigue damage. Mechanical dissipation can be deduced from the temperature changes captured on the tested specimen’s surface using infrared (IR) thermography. When mechanical dissipation is assumed to be spatially homogeneous in the tested specimen, processing can be performed using a macroscopic approach, also named zero-dimensional (0D) approach. This uses an averaged temperature over the whole specimen’s measurement zone. The reader is referred to Ref. ^[1] for a list of references in which the 0D approach is employed. This list can be updated with Ref. ^[2] dedicated to pure copper, Refs. ^[3,4] dedicated to rubber, and Ref. ^[5] dedicated to different types of leathers. The present study analyzes the error generated by the 0D approach in the assessment of mechanical dissipation due to fatigue loading. This error can be measured with respect to a one-dimensional (1D) approach, which is applicable to longitudinal specimens subjected to uniaxial tests. Both approaches are based on the heat diffusion equation:

- the 1D approach separately accounts for heat exchanges by convection with the ambient air, and those by conduction in the specimen. Note that the heat exchanges at the contact with the two grips of the testing machine are implicitly taken into account, as they derive from the temperature gradient at the two ends of the specimen through the Fourier law. The 1D approach was employed in Refs. ^[6,7] for steels, Refs. ^[8,9] for pure copper, Refs. ^[10,11] for shape-memory alloys and Ref. ^[12] for a polyamid;
- the 0D approach considers a “global” heat exchange with the outside of the tested specimen through the use of an averaged temperature over the specimen’s measurement zone. It can be applied when the heat which is produced or absorbed by the material is

spatially homogeneous in the specimen. Indeed, in that case the heat exchanged by contact with the jaws of the testing machine can be considered as nearly proportional to the mean temperature change.^[6] Considering the classically-accepted notion of proportionality for the heat exchanged by convection with the ambient air, the total heat exchanged with the environment (air + jaws) is thus also proportional to the mean temperature change. It is worth noting that homogeneity in the temperature fields is not required in the 0D approach.

Experimental tests and simulations were performed on pure copper and acrylic glass (PMMA), corresponding to extreme cases of thermal diffusivity. As in Ref. ^[1], the temperatures of two reference samples were used to track changes in the specimen's environment. Each reference sample was attached to one jaw of the testing machine, enabling us to reduce parasitic noise. Indeed, long tests (such as fatigue tests) are unavoidably accompanied by changes in the specimen's environment which penalize the mechanical dissipation assessment: an increase in the temperature of the testing machine during operation, potential modifications in the ambient air flow and temperature, and more generally in the elements of the testing room (persons, machines, etc). Similarly, Ref. ^[13] first employed a cooled actuated grip (using circulating water) and a dummy specimen (placed next to the specimen) to reduce the influence of the specimen's environment. Finally, it should be noted that the aim of the paper is not to provide a fatigue analysis of the two considered materials, but to estimate the relevancy of the 0D approach for these two materials.

The paper is organized as follows. Section 2 recalls the background of the 0D and 1D approaches for heat source calculation. Section 3 describes the experimental set-up in terms of materials, mechanical loading, and thermal acquisition conditions for mechanical dissipation measurement. Section 4 presents the experimental results obtained for pure copper and PMMA. A model to assess the error generated by the 0D approach is then developed in Section 5, for comparison purposes with respect to the experimental results. Concluding remarks close the paper concerning the relevance of the 0D approach for mechanical dissipation measurement.

2. Background on the two approaches used for heat source calculation

This section recalls the background of the present study. Let us consider a longitudinal thin plane specimen with constant cross-section, placed in the jaws of a uniaxial testing machine: see Fig. 1. Two reference samples are used to track variations in the specimen’s environment.^[1] Each of the references is clamped in one jaw of the machine to follow the temperature variations in the jaws. The references are made of the same material as the tested specimen. They can be separate pieces (see Fig. 1-a), or can form a monolithic piece with the mechanically tested part (see Fig. 1-b). The former configuration was tested in Ref. ^[1] to measure mechanical dissipation during the mechanical training of a shape-memory alloy. The latter configuration is here used for the first time.

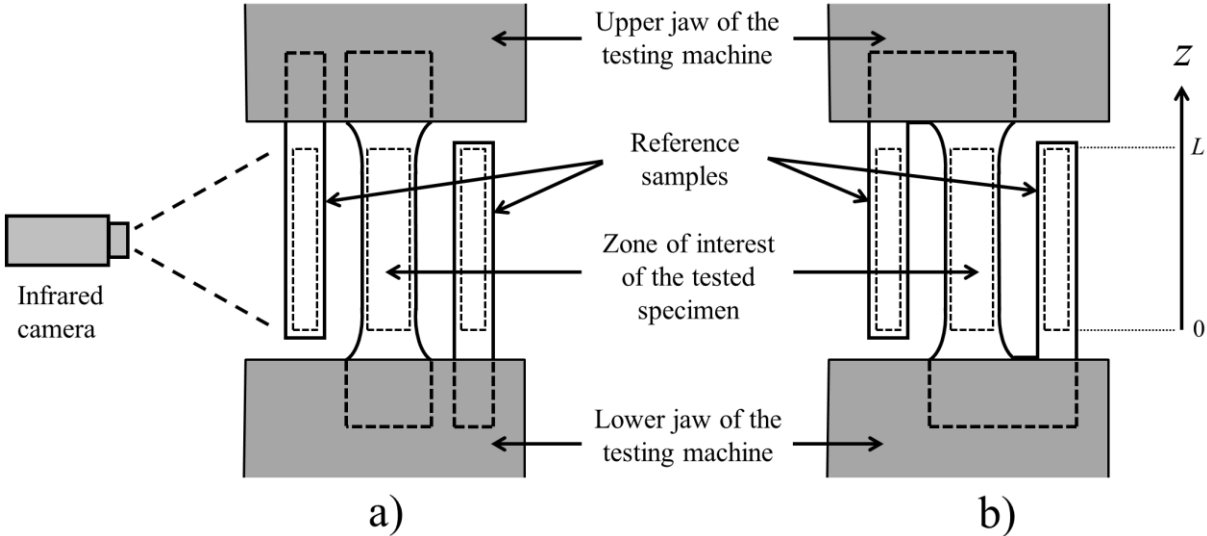


Figure 1 Schematic view of the experimental configurations proposed to assess the heat sources produced by a material specimen subjected to uniaxial loading. Two references are employed to follow variations in the specimen’s thermal environment.

Two thermal quantities are now introduced:

- $\Theta_{0D}(t)$ is the variation in the macroscopic temperature change;

- $\Theta_{1D}(z, t)$ is the variation in the vertical temperature change distribution ($z \in [0, L]$ where L is the length of the measured zone, see Fig. 1-b).

Both quantities are defined with respect to the mean temperature T_{ref} of the two reference samples as follows:

$$\Theta_{0D}(t) = \{T_{0D-spec}(t) - T_{0D-spec}(0)\} - \{T_{ref}(t) - T_{ref}(0)\} \quad (1)$$

$$\Theta_{1D}(z, t) = \{T_{1D-spec}(z, t) - T_{1D-spec}(z, 0)\} - \{T_{ref}(t) - T_{ref}(0)\} \quad (2)$$

where

- $T_{0D-spec}(t)$ is the variation in the temperature averaged over the specimen's measured zone;
- $T_{1D-spec}(z, t)$ is the variation in the vertical temperature change distribution. In practice, a horizontal averaging over the specimen's width can be applied to improve the thermal resolution;
- $T_{ref}(t)$ is the variation in the temperature averaged over the two reference zones.

The term “heat source” means the heat power density (in $W.m^{-3}$) that is produced or absorbed by the material due to a change in its thermomechanical state. The quantity is negative or positive when the material absorbs or produces heat, respectively. Several versions of the heat diffusion equation have been proposed in the literature for the direct calculation of the heat sources from the temperature changes: 2D, 1D and 0D versions exist.^[6] The latter case can be applied when the heat sources are spatially homogeneous in the specimen, *i.e.* without strain localization or fatigue damage localization. Let us denote $s(t)$ the variation over time t in the heat source, assumed here to be spatially homogeneous in the specimen (it does not depend on the vertical coordinate z along the specimen length, see Fig. 1-b). In that case, the following two versions of the diffusion equation can be proposed to calculate the (homogeneous) heat source s :

$$s = \rho C \left(\frac{d\Theta_{0D}}{dt} + \frac{\Theta_{0D}}{\tau_{0D}} \right) \quad (3)$$

$$s = \rho C \left(\frac{\partial \Theta_{1D}}{\partial t} + \frac{\Theta_{1D}}{\tau_{1D}} \right) - \lambda \frac{\partial^2 \Theta_{1D}}{\partial z^2} \quad (4)$$

where the material parameters are the density ρ , the specific heat C and the thermal conductivity coefficient λ , assumed to be homogeneous. Two time constants are considered to characterize the ability of the specimen to exchange heat with its environment:

- τ_{0D} for global heat exchanges with the jaws and the ambient air, to be used in the 0D approach;
- τ_{1D} for heat exchanges with the ambient air only, to be used in the 1D approach.

See Section 2 of Ref. ^[1] for some properties of the heat exchange constants. It can be noted that $\tau_{0D} < \tau_{1D}$ by definition. This inequality can be illustrated by considering a natural return to ambient temperature. This return is obviously quicker when the specimen is clamped in the jaws of the testing machine. Indeed, in that case the global heat losses (characterized by τ_{0D}) are the sum of the heat exchanges by convection with the air (characterized by τ_{1D}) and by contact with the jaws.

The heat source s is the sum of two calorific quantities:^[12]

- one part is the *mechanical dissipation*. It is often denoted d_1 to be distinguished from thermal dissipation d_2 , both quantities appearing in the Clausius-Duhem inequality $d_1 + d_2 \geq 0$. Mechanical dissipation is related to irreversibility such as plasticity, viscosity or fatigue damage. The calorific quantity is always positive: $d_1 \geq 0$;
- the second part is associated with *thermomechanical couplings*. For instance, phase transitions can accompany material stretching, leading to the production or absorption of latent heat. Typical examples are strain-induced crystallization in rubber and stress-induced transformation in shape memory alloys. More classically, thermo-elastic couplings exist in all materials. Two types of such a coupling can be distinguished, depending on the material elasticity.^[5] For isentropic elasticity, such as

in metals and polymers below their glass transition temperature, loading in tension is accompanied by heat absorption (temperature decrease), while unloading is accompanied by heat production (temperature increase). For entropic elasticity, such as in rubber-like materials or polymers above their glass transition temperature, the inverse phenomenon occurs. It is worth noting that, in all cases, the total heat due to thermomechanical couplings is null over a thermodynamic cycle. This property is useful when considering a cyclic loading.

Eqs. 1 and 3 were proposed and tested in Ref. ^[1] to assess homogeneous mechanical dissipation from the 0D approach during a cyclic test while reducing parasitic effects associated with changes in the specimen's environment. Eq. 2 is here coupled to Eq. 4 for the 1D assessment of the homogeneous mechanical dissipation produced by specimens subjected to uniaxial fatigue tests, for comparison with the results of the 0D approach.

3. Experimental set-up

A hydraulic 15 kN MTS testing machine was used for the fatigue tests (see Fig. 2-a). Its mobile grip was the upper one, leading to higher temperatures at the top of the specimen compared to its bottom. This is due to the actuator, whose lubricating oil produces heat that diffuses through the specimen. Temperature difference between the top and the bottom of a specimen can reach a few degrees. In practice, we ran the testing machine for three hours in cycling configuration (without a specimen) before starting the actual test, in order to approach a stabilized thermal configuration of the machine.

Figure 2-b shows the two types of specimen tested:

- copper specimens exhibiting a rectangular shape, 0.50 mm in thickness and 30 mm in width. The reference samples were two rectangular pieces distinct from the

mechanically-loaded part. The length L of the measured zone was equal to 60 mm, for a total distance between the jaws of 80 mm;

- PMMA specimens, 3 mm in thickness, comprising the mechanically-loaded part (10 mm in width) and the two references in a single piece. They were obtained by laser cutting. The length L of the zone of interest and the distance between the jaws were equal to 50 mm and 70 mm respectively.

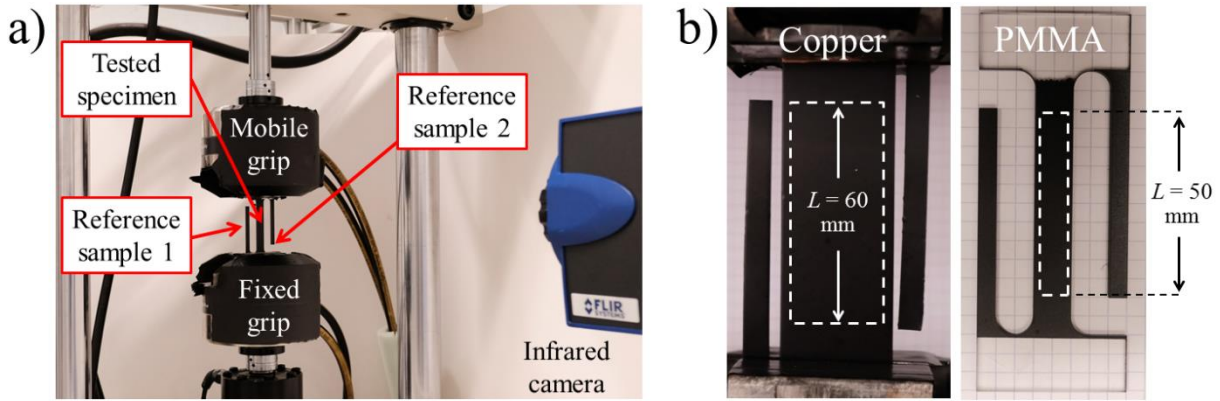


Figure 2 Experimental set-up: a) experiment; b) two types of tested specimens.

For both types of specimen, temperatures were measured using a Cedip Jade III-MWIR camera exhibiting a noise-equivalent temperature difference of 0.02 K. The spatial resolution of the temperature measurement, corresponding to the size of the IR pixel projected on the specimen's plane, was equal to 0.35 mm. To increase the thermal emissivity of the observed surfaces, a thin layer of matte black paint (emissivity of 0.95) was applied to the specimens and the two references. Black curtains were also placed around the specimen's immediate environment to reduce reflections in the IR wavelength range (not shown in Fig. 2-a).

Loading consisted of a sinusoidal force-controlled signal:

- for copper specimens, the loading frequency f_L was fixed at 60 Hz for 9,000 cycles (*i.e.* 150 s) before coming back to zero stress in 2 s. The maximum and minimum stresses were set to 120 MPa and 12 MPa respectively (stress ratio of 0.1);
- for PMMA specimens, the loading frequency f_L was set to 2 Hz. Four blocks of 1,600 cycles (*i.e.* 800 s) were applied. Maintaining a stress ratio of 0.1, the amplitudes $\Delta\sigma$

were set to 6.7 MPa, 13.4 MPa, 21.1 MPa and 26.8 MPa successively.

These choices resulted from different compromises. The higher loading frequency for copper (60 Hz) compared to PMMA (2 Hz) is due to the fact that heat exchanges with the outside environment are much faster for copper specimens than for PMMA specimens. Loading frequencies which are too small may lead to temperature changes which are difficult to detect, especially for metallic materials. Indeed, metals have high thermal conductivity, leading to rapid heat exchange with specimen's environment, especially by contact with the jaws of the testing machine. Similar considerations led us to use different loading durations (150 s for copper and 800 s for PMMA). Indeed, a steady-state thermal regime is reached more quickly in the case of copper because equilibrium between the heat produced and the heat exchanged occurs earlier. Preliminary tests enabled us to state that temperature changes of at least 0.1°C could be reached with the above loading conditions. In practice, the chosen conditions (frequencies, amplitudes and number of cycles) resulted from a compromise between machine capability and attainable amplitudes of temperature change. It should also be pointed out that the objective here is not to perform a fatigue analysis of the two considered materials. We only aim to compare the mechanical dissipations obtained by the 0D and 1D approaches.

The temperature acquisition conditions were such that they could enable us to directly extract the mechanical dissipation d_1 from the total heat source s .^[1] The camera acquisition frequency f_A was set to 100 Hz, but each image recorded was the average of 100 successive frames, leading to a recording frequency f_R of 1 Hz. Each recorded thermal image thus corresponded to the average of $n_R = f_L / f_R = 60$ mechanical cycles for copper, and of $n_R = f_L / f_R = 2$ mechanical cycles for PMMA. The temperature changes Θ_{0D} and Θ_{1D} were thus obtained at frequency $f_R = 1$ Hz using Eqs. 1 and 2 respectively. The heat source s was then calculated from Eqs. 3 or 4 using finite differences for the derivative terms. As the heat due to thermo-elastic coupling is null over an integer number of mechanical cycles, the obtained heat source s at frequency $f_R = 1$ Hz is equal to the mechanical dissipation averaged over $n_R = 60$ mechanical cycles for copper and over $n_R = 2$ mechanical cycles for PMMA. As demonstrated in Ref. [1], this property is actually true only if the temperature fluctuation is cyclic; that is to say in the “steady-state thermal regime”. Note,

however, that the difference between the obtained heat source s and mechanical dissipation in the transient regime is low compared to the amplitude of the thermo-elastic coupling heat sources. The next section presents the experimental assessment of the mechanical dissipation averaged over n_R mechanical cycles, still named d_1 in the following for the sake of simplicity, for the two materials considered.

4. Experimental assessment of mechanical dissipation and comparison between 0D and 1D approaches

This section presents the experimental results for the two tested materials and the comparison between the mechanical dissipation obtained with the 0D and 1D approaches. First, some tests were required to estimate the time constants characterizing the heat exchanges with the environment of the specimens placed in the jaws of the testing machine.

4.1. Preliminary characterization of τ_{0D} and τ_{1D}

Preliminary tests were performed to provide the necessary quantities for processing by Eqs. 3 and 4. For the 0D approach, the thermal data processing to calculate heat sources requires the knowledge of the material parameters ρ and C , as well as the time constant τ_{0D} , see Eq. 3. For the 1D approach, Eq. 4 also requires the value of λ , as well as the time constant τ_{1D} . The material parameters ρ , C and λ are taken from the literature (see Table 1), [14, 15, 16] while the two time constants τ_{0D} and τ_{1D} must be determined from a natural return to ambient temperature. Note that for PMMA, wide ranges of values are found in the literature for the product ρC (more than 10 percent variation) and for λ (more than 30 percent variation). For the identification of τ_{0D} , the test must be performed with the specimen placed in the jaws of the testing machine, as for the mechanical tests. During a natural return to ambient temperature, the heat source produced by the material is null: $s(t) = 0$. As a consequence, the solution of Eq. 3 is simply given by

$$\Theta_{0D}(t) = \Theta_{any} e^{\frac{-(t-t_{any})}{\tau_{0D}}} \quad (5)$$

where Θ_{any} is the temperature change at any time t_{any} . The heating mode (prior to the natural return to ambient temperature) was material self-heating by fatigue loading for a short duration. This choice is relevant because it better guarantees the homogeneous heating of the specimen's zone of interest than via external heating by contact or convection. Moreover, it creates temperature **variation** whose order of magnitude is the same as during the fatigue test to be performed afterwards.

For copper specimens, parameter τ_{0D} was identified as 7.6 s by mean square approximation of the experimental curve, see Fig. 3-a. Parameter τ_{1D} is also identified from a return to ambient temperature, but the specimen should not be placed in the jaws of the testing machine. The specimen was merely suspended in air from the top jaw with a small piece of adhesive tape, and initially heated with a hair dryer for a few seconds before returning to ambient temperature. τ_{1D} was assessed as 90 s, which is one order of magnitude greater than the value of τ_{0D} . This means that during a mechanical test, most of the heat losses are at the contacts between the copper specimen and the metallic jaws of the testing machine. It can be seen in Fig. 3-b that the temperature change distributions are strongly curved, due to these heat losses at the two ends of the specimen. A similar approach was used for PMMA specimens: see Table 1 for the values of τ_{0D} and τ_{1D} . It can be noted that parameter τ_{0D} is much greater for PMMA (160 s) than for copper (7.6 s). This result is logical for two reasons: first because of the small thermal conductivity of polymers compared to metals (longer duration for the heat to reach the boundaries of the specimen); second because of the slower heat exchanges with the jaws of the testing machine (metal/polymer contact). Moreover for PMMA, it can also be noted that τ_{1D} is only 1.16 greater than τ_{0D} ($185/160 = 1.16$, compared to $90/7.6 = 11.8$ for copper). This means that a large part of the heat is exchanged with the ambient air in the case of PMMA, whereas most of the heat is exchanged with the jaws of the testing machine in the case of copper.

Table 1 Parameters for pure copper and PMMA. Parameters ρ , C and λ are taken from the literature.^[14, 15, 16]

Parameter	For copper	For PMMA
Density, ρ	8960 kg/m ³	1170 kg/m ³
Specific heat, C	385 J/(kg.°C)	1465 J/(kg.°C)
Thermal conductivity coefficient, λ	401 W/(m.K)	0.2 W/(m.K)
Time constant for the 0D approach, τ_{0D}	7.6 s	160 s
Time constant for the 1D approach, τ_{1D}	90 s	185 s
Longitudinal heat exchange coefficient, h	∞	1.2 W/(m ² .K)

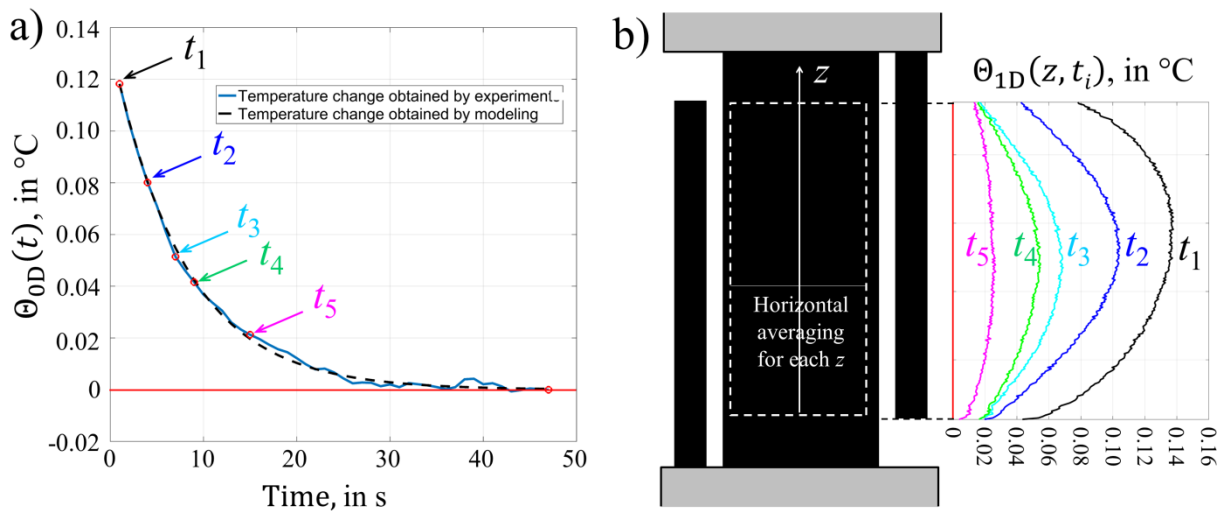


Figure 3 Natural return to ambient temperature of a copper specimen placed in the jaws of the testing machine: a) temperature change observed in the specimen's measurement zone as a function of time, b) temperature change profiles along the length of the specimen's measurement zone.

4.2. Results for pure copper

Figure 4-a shows the temperature change in the specimen's zone of interest as a function of time during the cyclic test described in Section 3, for pure copper. Let us recall that the

thermal acquisition conditions were such that each recorded thermal value corresponds to an average over 60 mechanical cycles. The following comments can be made concerning this figure:

- a small temperature drop ($\Theta_{0D} < 0$) is observed at the beginning of the test. It is caused by thermo-elastic coupling, which creates a negative heat source when the stress increases. Indeed, the cyclic loading *started* with a stress increase. Even if the thermo-elastic coupling heat is null over an integer number of mechanical cycles, it takes almost $3 \tau_{0D}$ from the beginning of the test to see a thermal response due mechanical dissipation only;^[1]
- a temperature increase is observed at the end of the test (corresponding to the return to zero stress in 2 s, see Section 3). Indeed, even if the stress rate is small compared to that of the fatigue phase (frequency $f_L = 60$ Hz), the effect of the thermo-elastic coupling is not “cancelled” by the temporal averaging as is the case in the fatigue phase. Let us recall that the stress ratio for cyclic tensile loading was equal to 0.1, thus the final unloading phase corresponded necessarily to a *negative* stress rate. A final return to zero stress from a compressive state (for instance after cyclic loading with a negative stress ratio, such as -1) would have led to a final temperature *decrease* because of a *positive* stress rate;
- after a transient regime lasting about 20 s ($\approx 3 \tau_{0D}$), the temperature stabilized. The mean value over the whole duration of the steady-state thermal regime was calculated to increase the measurement resolution of the stabilized temperature: it gives $(\Theta_{0D})_{\text{steady}} = 0.101^\circ\text{C}$.

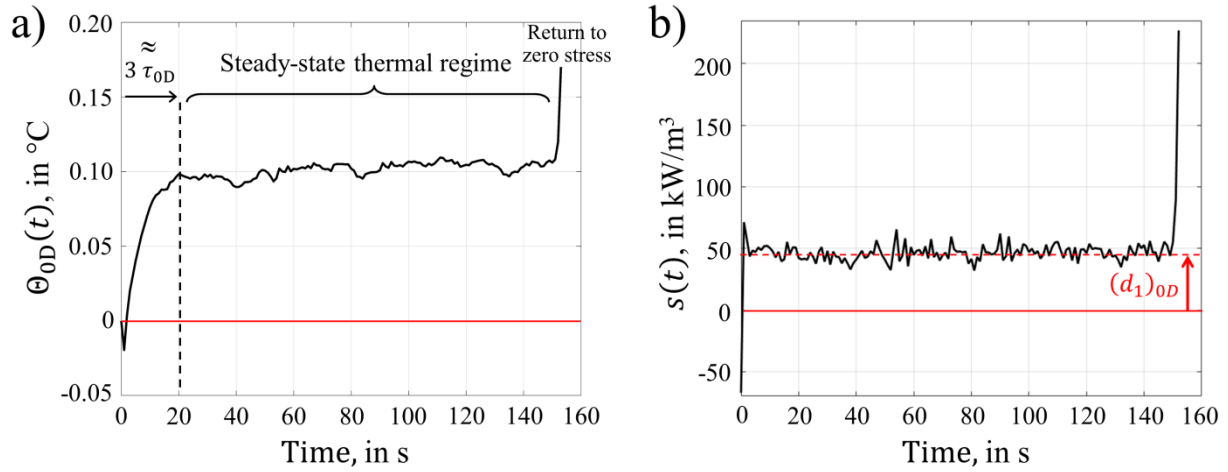


Figure 4 Result for the copper fatigue test (at 60 Hz) using the 0D approach: a) temperature change of the specimen's measurement zone as a function of time. Each thermal datum (recorded at a frequency of 1 Hz) corresponds to an average over 60 mechanical cycles, b) heat source as a function of time, calculated from Eq. 3.

Equation 3 was then applied to assess the mechanical dissipation from the 0D approach. Figure 4-b shows the heat source s as a function of time during the test. It can be noted that s is nearly constant during cyclic loading. The mean value of s over the duration of the cyclic loading is equal to $46.4 \text{ kW}/\text{m}^3$, providing a mean value for the mechanical dissipation $(d_1)_{0D}$. A simpler approach consists of directly considering the mean temperature change $(\Theta_{0D})_{\text{steady}}$ in the steady-state thermal regime, *i.e.*

$$(d_1)_{0D} = s(t > 3\tau_{0D}) = \rho C \left(0 + \frac{(\Theta_{0D})_{\text{steady}}}{\tau_{0D}} \right) = 45.8 \text{ kW}/\text{m}^3 \quad (6)$$

The difference with respect to the value $46.4 \text{ kW}/\text{m}^3$ can be explained by the slight mean temperature increase observed in the steady-state thermal regime in Fig. 4-a: an increase of about 0.02°C in 130 s, corresponding to a quantity $\rho C \frac{d\Theta_{0D}}{dt}$ equal to about $0.5 \text{ kW}/\text{m}^3$.

A remark can be made about the dimensions of the zone of interest which was used to extract the mean temperature change Θ_{0D} in the 0D approach. Indeed, as indicated in Section 3, the

considered length for the extraction zone was equal to 60 mm, whereas the total distance between the jaws was 80 mm (see Fig. 1-b). It is worth noting that the time constant τ_{0D} must be identified using the same extraction zone, as was the case in Section 4.1.

A comparison with the 1D approach is now proposed. Figure 5-a shows the temperature change distribution along the length of the copper specimen's zone of interest. The plotted profile is actually the average over the duration of the steady-state regime, to improve thermal measurement resolution. In order to improve the calorimetric measurement resolution, the mechanical dissipation assessment was performed at the center of the specimen, where the quantities Θ_{1D} and $\partial^2\Theta_{1D}/\partial z^2$ are the greatest over the specimen length, making the calculation on the terms in the right-hand side of Eq. 4 more reliable (greater signal-to-noise ratio). In practice, the central zone of the specimen (corresponding to 30% of the total length L) was considered for data extraction, especially the curvature $\partial^2(\Theta_{1D})_{\text{steady}}/\partial z^2$; see Fig. 5-a. This percentage of 30% of the total length L ensures the correct assessment of the curvature at the middle of the specimen. Percentages smaller than 30% lead to poor measurement of the curvature, while greater percentages are not relevant for an assessment localized at the middle of the specimen. The quantity $(\Theta_{1D})_{\text{steady}}$ was defined as the mean temperature change over this zone $z \in [0.35 L; 0.65 L]$: it gives $(\Theta_{1D})_{\text{steady}} = 0.140^\circ\text{C}$. The diffusion term was obtained from the curvature of the second-order polynomial function approximating the distribution over the same zone (see red curve in Fig. 5-b): it gives $\partial^2(\Theta_{1D})_{\text{steady}}/\partial z^2 = -110.6^\circ\text{C}/\text{m}^2$. Equation 4 was then used to calculate the mechanical dissipation d_1 from the 1D approach:

$$d_1 = s(t > 3\tau_{0D}) = \rho C \left(0 + \frac{(\Theta_{1D})_{\text{steady}}}{\tau_{1D}} \right) - \lambda \frac{\partial^2(\Theta_{1D})_{\text{steady}}}{\partial z^2} = 49.7 \text{ kW}/\text{m}^3 \quad (7)$$

Note that Θ_{1D} varies by about 0.01°C over the zone $z \in [0.35 L; 0.65 L]$ (see Fig. 5-b), corresponding to a variation in quantity $\rho C \Theta_{1D}/\tau_{1D}$ of about $0.4 \text{ kW}/\text{m}^3$, *i.e.* $\pm 0.2 \text{ kW}/\text{m}^3$ around the value $49.7 \text{ kW}/\text{m}^3$.

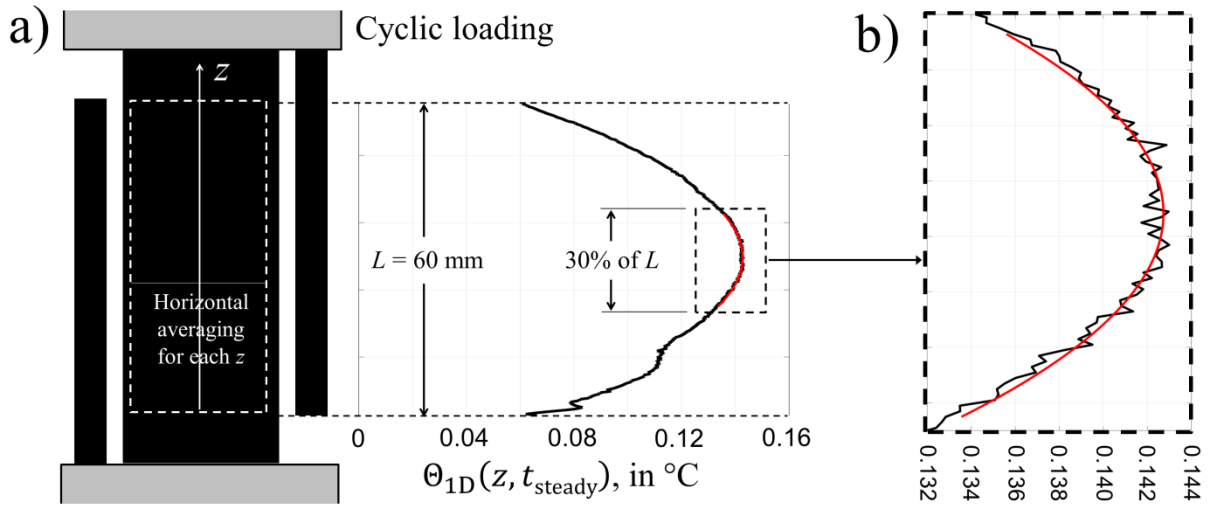


Figure 5 Result for the copper fatigue test using the 1D approach: a) temperature change distribution averaged over the steady-state duration, b) zoom into the central zone of the specimen and approximation by second-order polynomial function (in red).

By construction, mechanical dissipation is better estimated by the 1D approach than by the 0D approach. The error generated by the 0D approach can be then calculated as follows, in absolute and relative terms respectively:

$$E = (d_1)_{0D} - d_1 = -3.9 \text{ kW/m}^3 \quad (8)$$

$$E\% = \frac{(d_1)_{0D} - d_1}{d_1} \times 100 = -7.8 \text{ \%} \quad (9)$$

This error is small, but may be considered as non-negligible. Section 5 will provide a parametric analysis to analyze the influence of the material and the heat exchange properties on the error generated by the 0D approach.

4.3. Results for PMMA

Figure 6-a shows the temperature change $\Theta_{0D}(t)$ of the specimen's measured zone during the test, for PMMA. The following comments can be made concerning this figure:

- as expected, each of the four loading blocks starts with a small temperature drop (see, for instance, the zoom at the beginning of block #3). As was the case for copper, this is a consequence of thermo-elastic coupling each time the stress amplitude increases;
- after a transient regime, the temperature tends to stabilize. The attained temperature change $(\Theta_{0D})_{steady}$ increases at each block. The values of the mechanical dissipation $(d_1)_{0D}$ are then calculated from Eq. 3 in steady-state regime, similarly to what was done for Eq. 6 for copper: see Fig. 6-b. Logically, the higher the stress amplitude is, the higher the mechanical dissipation.

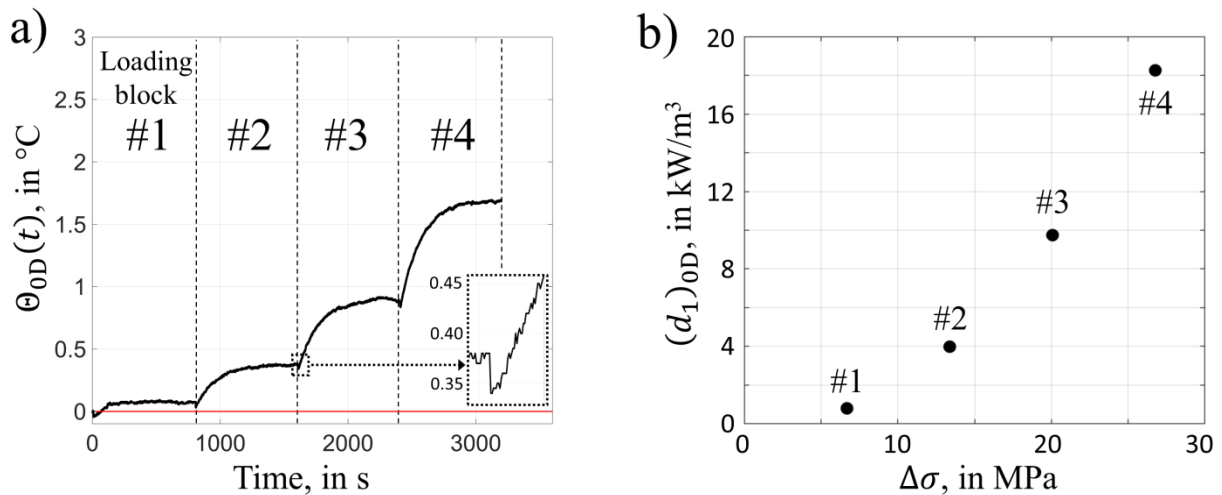


Figure 6 Result for the PMMA fatigue test (at 2 Hz) using the 0D approach: a) temperature change in the specimen's zone of interest as a function of time. Each thermal datum, recorded at a frequency of 1 Hz, corresponds to an average over 2 mechanical cycles; b) mechanical dissipation as a function of stress amplitude $\Delta\sigma$.

Figure 7 shows the steady temperature change distribution which is reached in each loading block. The profiles are quite flat for blocks #1 and #2, and curved for blocks #3 and #4.

Globally compared to Fig. 5, which corresponded to copper, the curvatures are small in the central zone of the specimen for all the blocks (which is expected because of the lower thermal conductivity of PMMA). The values for the mechanical dissipation d_1 were estimated using the 1D approach, as was done for copper in Eq. 7. Table 2 shows the results in terms of absolute error E and relative error $E\%$ generated by the 0D approach for each block. Two comments can be made from this table. First, the absolute error E slightly increases with the stress amplitude, but the order of magnitude remains quite similar. Second, the relative error $E\%$ strongly decreases when the stress amplitude increases, reaching 6.5% for the fourth block. The large relative errors for blocks #1 and #2 can be explained by the uncertainty in the assessment of the curvature $\partial^2(\Theta_{1D})_{\text{steady}}/\partial z^2$ in the central zone of the specimen, corresponding here to 30% of the length L . It can be also noted that the temperature distributions are not symmetrical: temperature changes are slightly higher in the upper part of the specimen. This convection effect may affect the quantitative results. In addition, uncertainty in the values of material parameters ρ , C and λ probably plays a role in the assessment of $E\%$. As for copper in Section 4.2, the error generated by the 0D approach may be considered as non-negligible for the elaboration of fatigue behavior laws.

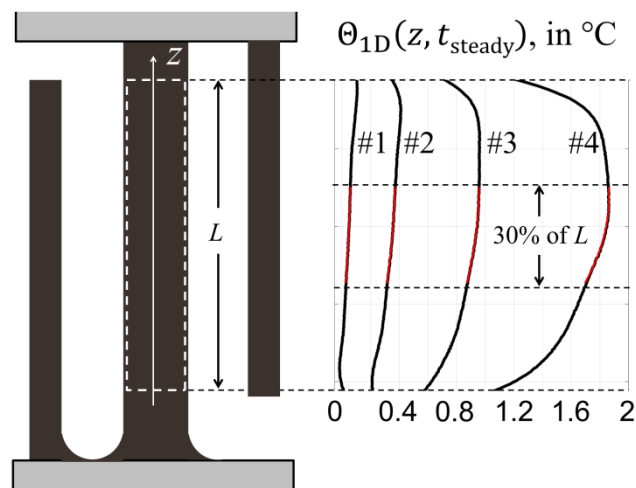


Figure 7 Result for the PMMA fatigue test using the 1D approach: temperature change distribution in the steady-state regime for loading blocks #1 to #4.

Table 2. Results for PMMA fatigue: error generated by the 0D approach in the estimation of the mechanical dissipation.

Block	Mechanical dissipation		Absolute	Relative
	0D approach	1D approach	Error	error
	$(d_1)_{0D}$	d_1	E	$E\%$
#1	0.76 kW/m ³	0.42 kW/m ³	0.34 kW/m ³	80 %
#2	3.9 kW/m ³	3.2 kW/m ³	0.7 kW/m ³	22 %
#3	9.6 kW/m ³	8.6 kW/m ³	1.0 kW/m ³	12 %
#4	17.9 kW/m ³	16.8 kW/m ³	1.1 kW/m ³	6.5 %

5. Modeling to assess the error generated by the 0D approach

5.1. Theoretical expressions for mechanical dissipation

A numerical tool was developed to study the error generated by the 0D approach in mechanical dissipation assessment. For this purpose, a 1D model was implemented. The input data are the material parameters ρ , C and λ , the length L of the specimen, the time constant τ_{1D} , as well as the mechanical dissipation d_1 . Note that an additional parameter will be introduced concerning the thermal boundary conditions at the two ends of the specimen (see Eq. 11 below). The output data is the mechanical dissipation $(d_1)_{0D}$ assessed by the 0D approach, enabling us to calculate the absolute error E and relative error $E\%$ compared to the input data d_1 . The calculation was performed in three steps.

Step 1: determination of the analytical expression of $(\Theta_{0D})_{steady}$ in fatigue.

Let us consider the steady-state regime of the 1D version of the heat diffusion equation (Eq. 4) for constant and homogeneous mechanical dissipation d_1 :

$$d_1 = \rho C \frac{(\Theta_{1D})_{\text{steady}}}{\tau_{1D}} - \lambda \frac{\partial^2 (\Theta_{1D})_{\text{steady}}}{\partial z^2} \quad (10)$$

For the sake of legibility in following equations, let us place the origin of the z -axis in the middle of the specimen: $z \in [-L/2; +L/2]$. For the boundary conditions, we consider heat losses that are proportional to the temperature change:

$$- \lambda \frac{\partial (\Theta_{1D})_{\text{steady}}}{\partial z} \left(\pm \frac{L}{2} \right) = h \times (\Theta_{1D})_{\text{steady}} \left(\pm \frac{L}{2} \right) \quad (11)$$

where h is a heat exchange coefficient expressed in $W/(m^2.K)$. Note that the case $\Theta_{1D}(\pm L/2) = 0$ corresponds to $h = \infty$. The solution to Eqs. 10-11 is given by:

$$(\Theta_{1D})_{\text{steady}}(z) = \frac{d_1}{\lambda \beta^2} \left[1 - \frac{\cosh(\beta z)}{\cosh\left(\beta \frac{L}{2}\right) \left[1 + \frac{\lambda \beta}{h} \tanh\left(\beta \frac{L}{2}\right)\right]} \right] \quad (12)$$

where

$$\beta = \sqrt{\frac{\rho c}{\lambda \tau_{1D}}} \quad (13)$$

In Eq. 12, the term $d_1/(\lambda \beta^2)$ corresponds to the temperature change in the middle of the specimen. The 0D version of the temperature change $(\Theta_{0D})_{\text{steady}}$ is then given by the averaged value of Θ_{1D} over the whole specimen length:

$$(\Theta_{0D})_{\text{steady}} = \frac{1}{L} \int_{-\frac{L}{2}}^{\frac{L}{2}} (\Theta_{1D})_{\text{steady}} dz = \frac{d_1}{\lambda \beta^2} \left[1 - \frac{2}{\beta L} \times \frac{\tanh\left(\beta \frac{L}{2}\right)}{1 + \frac{\lambda \beta}{h} \tanh\left(\beta \frac{L}{2}\right)} \right] \quad (14)$$

The calculation of $(d_1)_{0D}$ requires knowledge of the time constant τ_{0D} , which is calculated in the next step.

Step 2: determination of τ_{0D} during a natural return to ambient temperature

The 0D version of the heat equation during a natural return to ambient temperature ($s = 0$) is obtained by averaging Eq. 4 over the length L , and by taking into account the boundary conditions (Eq. 11) when the diffusion term is integrated. It gives:

$$0 = \rho C \left[\frac{\partial \Theta_{0D}}{\partial t}(t) + \frac{\Theta_{0D}(t)}{\tau_{1D}} \right] - \frac{2 h}{\rho C L} \Theta_{1D} \left(\pm \frac{L}{2}, t \right) \quad (15)$$

It is worth noting that $\Theta_{1D}(z, t)$ depends on the initial temperature distribution at $t = 0$ when starting the natural return to ambient. In experiments, $\Theta_{1D}(z, t = 0)$ is potentially heterogeneous because the specimen is placed in the jaws of the testing machine. Two cases can be considered.

For high values for the longitudinal heat exchange coefficient h in Eq. 11, let us say $h \gg \lambda/L$ (typically a metallic specimen clamped in metallic jaws), a numerical strategy was developed to find an empirical expression for τ_{0D} . An implicit Euler scheme of the 1D heat diffusion equation (Eq. 4) was considered to obtain synthetic values of $\Theta_{1D}(z, t)$ in two phases, similarly to the experimental procedure:

- phase 1: homogeneous heating ($s = \text{constant}$) for a short time;
- phase 2: natural return to ambient temperature ($s = 0$).

τ_{0D} is to be identified in phase 2 by considering the variation in time of the mean temperature change. Parameter h in Eq. 11 was set to infinity for the simulations. The numerical study has shown that τ_{0D} can be empirically expressed in the following form

$$\tau_{0D} \approx \alpha L^\gamma \tau_{1D}^\delta \quad (16)$$

where α , γ and δ are three constants depending on the material. Table 3 gives the values of these constants identified for $L \in [0.001; 0.2]$ m and $\tau_{1D} \in [1; 200]$ s. Identification was performed for pure copper, and also for aluminum alloys, steels and titanium alloys for future

use in other works. Note that γ and δ are both positive, meaning that τ_{0D} increases with L and/or τ_{1D} , which is logical.

Table 3. Values of the three parameters involved in the empirical expression of the time constant τ_{0D} (see Eq. 16). Identification of the parameters was performed numerically for $L \in [0.001; 0.2]$ m and $\tau_{1D} \in [1; 200]$ s.

Material	α	γ	δ
Pure copper	61.7	1.65	0.373
Aluminum alloys	55.4	1.64	0.439
Steels	18.5	1.07	0.684
Titanium alloys	6.52	0.68	0.82

For small values for the longitudinal heat exchange coefficient h , let us say $h \ll \lambda/L$, a simpler approach can be applied. Indeed, the temperature change distribution tends to flatten over time during the return to ambient. So we can write: $\Theta_{1D}(\pm L/2, t) \approx \Theta_{0D}(t)$. Identifying Eq. 15 with Eq. 3, it comes:

$$\tau_{0D} \approx \frac{1}{\frac{1}{\tau_{1D}} - \frac{2h}{\rho c L}} \quad (17)$$

Step 3: determination of the expression of $(d_1)_{0D}$ and mapping of the error compared with d_1

The expression of the mechanical dissipation in the 0D approach is given by Eq. 3 in a thermal steady-state regime. For high values for the longitudinal heat exchange coefficient h this gives, using Eqs. 14 and 16:

$$(d_1)_{0D} = \frac{1 - \frac{2}{\beta L} \tanh\left(\beta \frac{L}{2}\right)}{\alpha L^\gamma \tau_{1D}^{\delta-1}} \times d_1 \quad (18)$$

Then the absolute error and relative error for the mechanical dissipation assessment are defined respectively by

$$E = \frac{1 - \frac{2}{\beta L} \tanh\left(\beta \frac{L}{2}\right)}{\alpha L^\gamma \tau_{1D}^{\delta-1}} d_1 - d_1 \quad (19)$$

$$E\% = \left[\frac{1 - \frac{2}{\beta L} \tanh\left(\beta \frac{L}{2}\right)}{\alpha L^\gamma \tau_{1D}^{\delta-1}} - 1 \right] \times 100 \quad (20)$$

Similarly, for small values for the longitudinal heat exchange coefficient h this gives, using Eqs. 14 and 17:

$$(d_1)_{0D} = \left(1 - \frac{2 h \tau_{1D}}{\rho c L}\right) \left[1 - \frac{2}{\beta L} \times \frac{\tanh\left(\beta \frac{L}{2}\right)}{1 + \frac{\lambda \beta}{h} \tanh\left(\beta \frac{L}{2}\right)}\right] \times d_1 \quad (21)$$

$$E = \left(1 - \frac{2 h \tau_{1D}}{\rho c L}\right) \left[1 - \frac{2}{\beta L} \times \frac{\tanh\left(\beta \frac{L}{2}\right)}{1 + \frac{\lambda \beta}{h} \tanh\left(\beta \frac{L}{2}\right)}\right] d_1 - d_1 \quad (22)$$

$$E\% = \left\{ \left(1 - \frac{2 h \tau_{1D}}{\rho c L}\right) \left[1 - \frac{2}{\beta L} \times \frac{\tanh\left(\beta \frac{L}{2}\right)}{1 + \frac{\lambda \beta}{h} \tanh\left(\beta \frac{L}{2}\right)}\right] - 1 \right\} \times 100 \quad (23)$$

5.2. Analysis

The influence of the material and the heat exchanges with the specimen's environment is now discussed. First, Equation 20 was used to identify the influence of the length L and the time constant τ_{1D} on the relative error $E\%$ for pure copper. Figure 8 presents the map of $E\%$ for

$L \in [0.001; 0.2]$ m and $\tau_{1D} \in [1; 200]$ s. The following conclusions can be drawn from this figure:

- the relative error $E\%$ generated by the 0D approach strongly varies in the (L, τ_{1D}) plane. It can be positive or negative. Specimens which are too long, and/or heat exchanges by convection which are too strong, lead to a mechanical dissipation $(d_1)_{0D}$ which is underestimated. Either excessively short specimens or excessively weak convective exchanges lead to the same effect. There exist configurations for which the error is null;
- the experimental configuration of Section 4.2 is indicated by a cross on the graph. Note that the length to be considered here must be the distance between the upper and lower jaws of the testing machine, *i.e.* 80 mm. The theoretical relative error is equal to -15%, to be compared with the experimental value -7.8% (see Eq. 9). Considering the modeling hypotheses and the wide variation of $E\%$ in the (L, τ_{1D}) plane, it can be said that the experimental and simulated results are in fair agreement.

Similar trends were obtained using Eq. 20 for the other metals in Table 3. The analysis of a material featuring a low thermal diffusivity coefficient is presented in the next section.

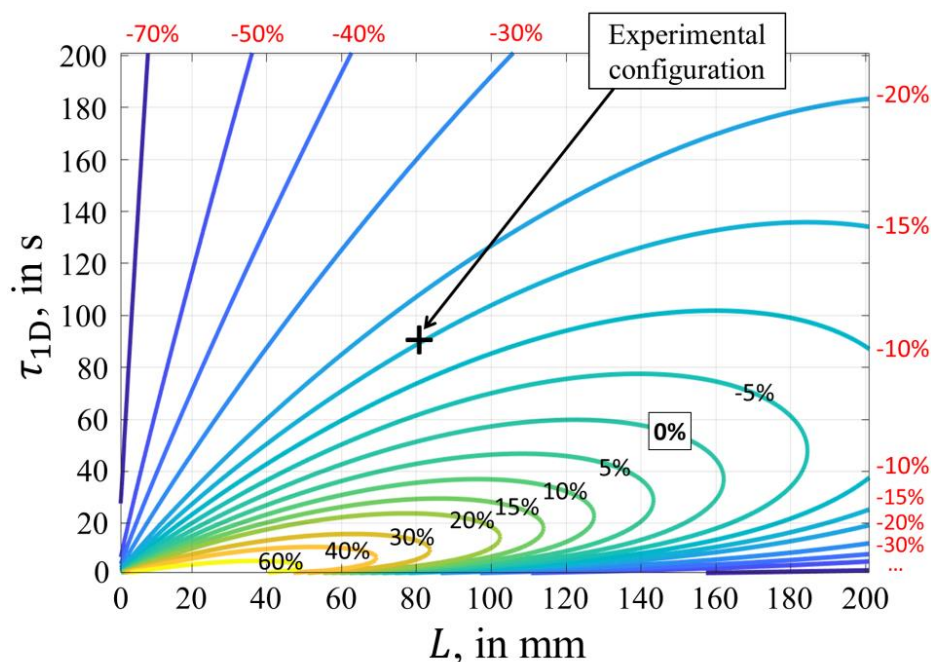


Figure 8 Modeling result for fatigue in copper: relative error $E\%$ on the mechanical dissipation assessment using the OD approach as a function of the specimen length L and the time constant τ_{1D} (see Eq. 20).

In the case of a small value for the longitudinal heat exchange coefficient h , the influence of the length L and the time constant τ_{1D} on the relative error $E\%$ can be discussed from Equation 23. Figure 9 presents the map of $E\%$ for PMMA for $L \in [0.001; 0.2]$ m, $\tau_{1D} \in [1; 200]$ s and $h = 1.2$ W/(m².K). The value of coefficient h was identified at the two ends of the measurement zone for blocks #3 and #4 for PMMA (see Fig. 7). The following comments can be made concerning Fig. 9:

- the relative error $E\%$ generated by the OD approach is always negative. It is interesting to note that $E\%$ quickly tends to zero when L increases;
- the experimental configuration of Section 4.3 is indicated by a cross on the graph, where the length to be considered is the distance between the upper and lower jaws, *i.e.* 70 mm. The theoretical relative error is equal to -0.6%, which is much smaller than the experimental errors in Table 3. Three reasons can be proposed to explain the discrepancy between the theoretical and experimental values of $E\%$. First, differences may be explained by an error in the modeling of the heat exchanges at the boundary conditions (see Eq. 11): the notion of proportionality between heat loss and temperature change at the contacts is indeed questionable. Thermal modeling using finite elements, including both specimen and jaws, could lead to a better estimation of the heat losses at the specimen's boundaries. Second, the ratio λ/L is about 3 W/(m².K), which is not significantly greater than the value of the longitudinal heat exchange coefficient h , meaning that the condition $h \ll \lambda/L$ is not really attained. Indeed, it is clearly observed for blocks #3 and #4 in Fig. 7 that the temperature profiles are considerably curved. Finally, discrepancy between the theoretical and experimental results may be also explained by uncertainty about the values of the density ρ , the specific heat C and the thermal conductivity coefficient λ . More precisely, the results depend on the ratio $\lambda/(\rho C)$. Let us recall that a wide range of values can be found in the literature for the

three parameters ρ , C and λ . Identification of these parameters could probably reduce the difference between the experimental and theoretical values of the relative error $E\%$;

- however, two general recommendations can be given for mechanical dissipation assessment for low thermal diffusivity materials. First, the longer the specimen, the more precise the 0D approach should be. Second, the greater the self-heating amplitude, the more precise the 0D approach should be, too. This can be done by increasing the loading frequency (although this may modify the material's fatigue response due to viscosity or other time-dependent effects).

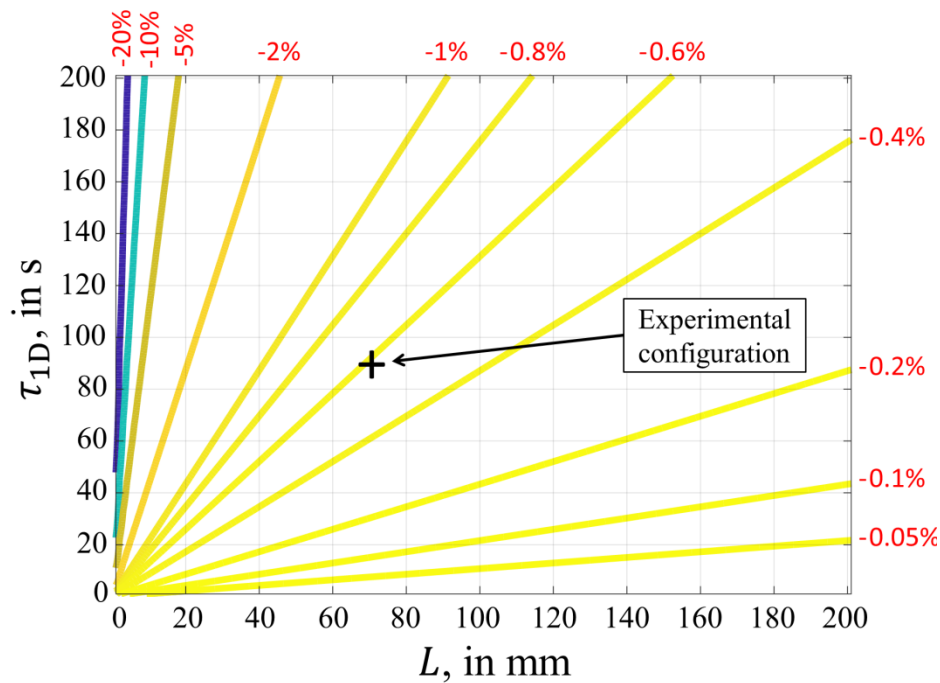


Figure 9 Modeling result for fatigue in PMMA: relative error $E\%$ for the mechanical dissipation assessment using the 0D approach as a function of the specimen length L and the time constant τ_{1D} (see Eq. 23).

6. Conclusion

The aim of this study was to analyze the error generated by the 0D approach in the assessment of mechanical dissipation in homogeneous specimens subjected to cyclic uniaxial tests. Results

were discussed from experiments based on infrared thermography, as well as from a model based on the 1D version of the heat diffusion equation and adequate averaging operations. The following conclusions can be drawn from the study:

- for metallic materials, the results showed that the error generated by the 0D approach may not be negligible. The error strongly varies, depending on the specimen's length and on the parameter τ_{1D} characterizing heat exchanges by convection with the air. The relative error can be positive or negative. There exist configurations for which the error is null. Specimens which are too long and/or heat exchanges by convection which are too strong lead to a mechanical dissipation which is underestimated by the 0D approach. The same is true for either particularly short specimens or particularly weak convective exchanges;
- for low thermal diffusivity materials, modeling showed that the error generated by the 0D approach quickly tends to zero when the specimen's length increases. Furthermore, the higher the material's self-heating is, the more precise the 0D approach for assessing the mechanical dissipation.

The 0D approach is a powerful tool for the thermomechanical analysis of materials, at least when heat sources are spatially homogeneous. Its use is quite simple, since it requires a "mean" temperature value. The present study showed that the error generated by this approach in mechanical dissipation measurement may not be negligible, and that careful attention must be paid to its application in fatigue analysis.

A perspective is the application to aluminum alloys, steels and titanium alloys. Besides continuum materials, the application of this study to granular materials like sands is another perspective, with the objective of identifying mechanical dissipation due to interparticle friction. Even if discrete systems are heterogeneous by nature, the heat sources can be expected to be homogeneous at the macroscopic scale, making the 0D approach applicable.

References

- [1] D. Delpueyo, X. Balandraud, M. Grédiac, S. Stanciu, N. Cimpoesu. A specific device for enhanced measurement of mechanical dissipation in specimens subjected to long-term tensile tests in fatigue. *Strain* **2018**, *54*, e12252
- [2] X.G. Wang, V. Crupi, C. Jiang, E.S. Feng, E. Guglielmino, C.S. Wang. Energy-based approach for fatigue life prediction of pure copper. *Int. J. Fatigue* **2017**, *104*, 243
- [3] J.B. Le Cam. Energy storage due to strain-induced crystallization in natural rubber: The physical origin of the mechanical hysteresis. *Polymer* **2017**, *127*, 166
- [4] J.B. Le Cam. Strain-induced crystallization in rubber: A new measurement technique. *Strain* **2018**, *54*, 12256
- [5] G. Corvec, N. Di Cesare, X. Balandraud, J.B. Le Cam, J. Gauffreteau. Thermomechanical characterization of leathers under tension using infrared thermography. *J. Mater. Sci.* **2019**, *54*, 862
- [6] A. Chrysochoos, H. Louche. An infrared image processing to analyse the calorific effects accompanying strain localisation. *Int. J. Eng. Sci.* **2000**, *38*, 1759
- [7] N. Connesson, F. Maquin, F. Pierron. Experimental energy balance during the first cycles of cyclically loaded specimens under the conventional yield stress. *Exp. Mech.* **2011**, *51*, 23
- [8] A. Blanche, A. Chrysochoos, N. Ranc, V. Favier. Dissipation assessments during dynamic very high cycle fatigue tests. *Exp. Mech.* **2015**, *55*, 699
- [9] N. Ranc, A. Blanche, D. Ryckelynck, A. Chrysochoos. POD preprocessing of IR thermal data to assess heat source distributions. *Exp. Mech.* **2015**, *55*, 725
- [10] X. Balandraud, A. Chrysochoos, S. Leclercq, R. Peyroux. Influence of the thermomechanical coupling on the propagation of a phase change front, *C. R. Acad. Sci. - Series IIB Mec.* **2001**, *329*, 621
- [11] V. Delobelle, D. Favier, H. Louche, N. Connesson. Determination of local thermophysical properties and heat of transition from thermal fields measurement during drop calorimetric experiment. *Exp. Mech.* **2015**, *55*, 711
- [12] B. Wattrisse, J.-M. Muracciole, A. Chrysochoos. Thermomechanical effects accompanying the localized necking of semi-crystalline polymers. *Int. J. Therm. Sci.* **2002**, *41*, 422

- [13] F. Maquin, F. Pierron. Heat dissipation measurements in low stress cyclic loading of metallic materials: From internal friction to micro-plasticity. *Mech. Mater.* **2009**, *41*, 928
- [14] Goodfellow. Metals, Alloys, Compounds, Ceramics, Polymers, Composites. Catalogue 1993/94
- [15] M.F. Ashby, Materials selection in mechanical design (Fourth Edition). Butterworth-Heinemann, Oxford, 2011
- [16] C.A. Harper, Handbook of Plastic Processes, John Wiley & Sons, Hoboken, NJ, USA, 2006